Oncogene (2014) **33,** 1713–1724

www.nature.com/onc

ORIGINAL ARTICLE

BAG3 induction is required to mitigate proteotoxicity via selective autophagy following inhibition of constitutive protein degradation pathways

F Rapino[1], M Jung[2] and S Fulda[1]

Simultaneous inhibition of the two major constitutive protein quality control (PQC) pathways, that is, the ubiquitin-proteasome system (UPS) and the aggresome-autophagy system, has been suggested as a promising strategy to trigger cell death in cancer cells. However, we observed that one third of rhabdomyosarcoma (RMS) cells survives parallel inhibition of the UPS by Bortezomib and the aggresome-autophagy pathway by the cytoplasmic histone deacetylase 6 inhibitor ST80, and is able to regrow upon drug removal, thus pointing to the induction of compensatory pathways. Here, we identify Bcl-2-associated athanogene 3 (BAG3) as a critical mediator of inducible resistance in surviving cells after concomitant blockage of constitutive PQC pathways by mitigating ST80/Bortezomib-triggered proteotoxicity via selective autophagy. ST80/Bortezomib cotreatment upregulates BAG3 mRNA and protein levels in surviving cells in addition to triggering the accumulation of insoluble protein aggregates. Intriguingly, knockdown of BAG3 by RNA interference severely impairs clearance of protein aggregates, significantly increases cell death and reduces long-term survival and clonogenic growth during recovery after ST80/Bortezomib cotreatment. Similarly, inhibition of autophagy by inducible autophagy-related protein 7 knockdown prevents removal of protein aggregates and cell regrowth during recovery after ST80/Bortezomib cotreatment. Also, the inhibition of lysosomal degradation using the V-ATPase pump inhibitor Bafilomycin A1 enhances accumulation of protein aggregates, and completely abolishes regrowth after Bortezomib/ST80-induced proteotoxic stress. By identifying BAG3 as a key mediator of inducible resistance by mitigating proteotoxicity via selective autophagy after inhibition of constitutive PQC systems, our study provides new insights into the regulation of PQC pathways in cancer cells and identifies new targets for therapeutic intervention.

Oncogene (2014) **33,** 1713–1724; doi:10.1038/onc.2013.110; published online 6 May 2013

Keywords: BAG3; autophagy; proteasome inhibitor; HDAC6; cancer

INTRODUCTION

Protein quality control (PQC) is tightly regulated in mammalian cells by both constitutive and inducible systems in order to avoid proteotoxicity of accumulated misfolded or insoluble proteins, and to sustain cellular growth.[1] Under basal conditions, PQC is predominately carried out by the following two mechanisms: First, the ubiquitin-proteasome system (UPS) is responsible for the degradation of linearized and ubiquitin-tagged proteins.[1] Second, the aggresome-autophagy system mediates degradation of insoluble protein aggregates and aggresomes.[1] In the aggresomal-autophagic degradation pathway, the cytoplasmic histone deacetylase 6 (HDAC6) is required for the dynein-mediated, retrograde transport of protein aggregates along microtubules to the microtubule organizing center to form aggresomes by binding to ubiquitin-tagged proteins and by deacetylating α-tubulin.[2] In addition, HDAC6 is necessary for autophagosomal maturation and the clearance of protein aggregates and aggresomes via autophagy. To this end, HDAC6 recruits cortactin via deacetylation, thereby promoting the formation of an F-actin network that supports autophagosome-lysosome fusion.[3]

Autophagy is an evolutionarily conserved, ubiquitous and multi-step process, by which cytosolic material is sequestered in a double-layered membrane, delivered to the lysosome for degradation and recycled to fuel cellular growth.[4] Autophagy starts with the formation of an isolation membrane, a double membrane structure also called phagophore, which then encapsulates cytoplasmatic cargo, seals to form the autophagosome and eventually fuses with lysosomes to generate autophagolysosomes, where the cargo is broken down into its constituent components.[4] While autophagy has for long been considered as a bulk degradation process, the recent discovery of several autophagy receptor proteins, including p62 revealed that autophagy can also occur in a selective manner.[5] p62 links protein aggregates to the autophagic machinery by binding on one side via its ubiquitin-associated domain to ubiquitin-tagged proteins and on the other side via its LC3-interacting region domain to the autophagosomal membrane protein LC3-II.[6] By recruiting protein aggregates or aggresomes as cargo to autophagic membranes to form autophagosomes, p62 promotes their degradation.[6] In addition, p62 itself is a substrate for autophagic degradation and accumulates upon inhibition of autophagy.[6]

[1]Institute for Experimental Cancer Research in Pediatrics, Goethe-University, Frankfurt, Germany and [2]Institute of Pharmaceutical Sciences, Albert-Ludwigs-University, Freiburg, Germany. Correspondence: Professor Dr S Fulda, Institute for Experimental Cancer Research in Pediatrics, Goethe-University, Komturstr. 3a 60528, Frankfurt, Germany.
E-mail: simone.fulda@kgu.de
Received 1 November 2012; revised 21 January 2013; accepted 7 February 2013; published online 6 May 2013

When constitutive PQC is compromised, the inducible branch of PQC is usually activated as an on-demand, compensatory mechanism to ensure PQC.[7] For example, during aging when the activity of the proteasome declines, a transcriptional switch from Bcl-2-associated athanogene 1 (BAG1)-regulated protein degradation via the proteasome to BAG3-dependent selective autophagy has recently been described.[8] BAG3 is a co-chaperone of the BAG family (BAG1-6) and binds to chaperone proteins such as HSP70 and HSPB8, which allows the recognition and binding to misfolded substrates.[9] Furthermore, BAG3 stimulates substrate transfer from HSP70 to the dynein motor complex by acting as a nucleotide-exchange factor, thereby facilitating the dynein-mediated retrograde transport of misfolded proteins to the microtubule organizing center to form aggresomes.[8] In addition, BAG3 promotes selective autophagy via its interaction with p62.[8]

Given the importance of proper PQC to maintain cell viability, these pathways have been exploited as therapeutic targets in oncology.[10] For example, Bortezomib, a reversible proteasome inhibitor, demonstrated potent *in vitro* and *in vivo* antitumor activity against various hematological malignancies and solid cancers, and is approved for the treatment of certain tumors, for example, multiple myeloma.[10] However, several cancers exhibit primary or acquired resistance to Bortezomib-based therapies, thus calling for new strategies to bypass this resistance. For example, engagement of the aggresome-autophagy system has been encountered as a defense mechanism to compensate as alternative constitutive PQC pathway for inhibition of the UPS. Therefore, proteasome inhibitors have been combined with HDAC inhibitors to concomitantly inhibit the two key constitutive protein degradation pathways in order to increase the antitumor activities of proteasome inhibitors.[11–13]

In rhabdomyosarcoma (RMS), the most common pediatric soft tissue tumor, initial studies showed that Bortezomib triggers cell death *in vitro* and *in vivo*.[14] Therefore, we used RMS cells as a model to study the regulation of constitutive and inducible protein degradation pathways. Specifically, we asked whether simultaneous inhibition of both the UPS and the aggresome-autophagy pathway, in addition to synergistically inducing cell death, engages inducible PQC pathways as escape mechanism in surviving cells in order to overcome proteotoxicity.

RESULTS

A subpopulation of RMS cells survives and recovers after ST80/Bortezomib cotreatment

Initially, we asked whether simultaneous inhibition of the two major protein degradation pathways, that is, the UPS and the aggresome-autophagy system, co-operates to trigger cell death in RMS cells via increased proteotoxic stress. To address this question, we used the effect of the proteasome inhibitor Bortezomib and the selective HDAC6 inhibitor ST80.[15] Importantly, the addition of ST80 significantly increased Bortezomib-induced apoptosis in different RMS cell lines as determined by DNA fragmentation as a parameter of apoptosis (Figure 1a). In contrast to RMS cells, ST80 did not enhance Bortezomib-induced cell death in non-transformed human fibroblasts (Figure 1a), pointing to some tumor selectivity.

In addition to this co-operative induction of cell death upon cotreatment with ST80/Bortezomib, we also noticed that a substantial subpopulation (about one third) survived cotreatment with ST80/Bortezomib (Figure1b). To explore whether these surviving cells were able to recover upon drug removal, we monitored cell viability for several days after the removal of ST80 and Bortezomib (Supplementary Figure S1a), which are reversible inhibitors, using both an embryonal (RD) and alveolar (RMS13) RMS cell line. Interestingly, cells that survived cotreatment with ST80/Bortezomib regrew after drug removal at a similar rate as untreated cells (Figure 1c). This suggests that a defense mechanism is induced in response to treatment with ST80/Bortezomib, which decreases proteotoxicity and supports cell recovery. In the present study, we therefore aimed at identifying the molecular basis of this inducible escape mechanism.

ST80/Bortezomib cotreatment triggers accumulation of insoluble protein aggregates

As inhibition of the proteasome or HDAC6 has previously been shown to cause accumulation of ubiquitin-positive, insoluble protein aggregates,[16,17] we analyzed protein aggregates upon treatment with ST80 and/or Bortezomib by fractioning cell lysates in TritonX-100 soluble and insoluble fractions. Of note, we detected a marked increase of ubiquitinated protein aggregates in the insoluble fraction in cells cotreated with ST80/Bortezomib (Figure 2a). In parallel, ST80/Bortezomib cotreatment caused an increase of p62 protein levels in the insoluble fraction, a typical substrate of autophagic degradation (Figure 2a). Also, we used the filter trap assay as an alternative method to analyze protein aggregates. Similarly, cotreatment with ST80/Bortezomib caused accumulation of ubiquitin-positive protein aggregates compared with treatment with ST80 or Bortezomib alone (Supplementary Figure S1b).

To investigate whether this accumulation of protein aggregates is due to dysfunction of autophagy in surviving cells, we assessed the conversion of LC3 from the cytosolic form, that is LC3-I, to the autophagosome-associated form, that is, LC3-II. Of note, the conversion of LC3-I to LC3-II was not impaired in ST80/Bortezomib-cotreated cells (Figure 2b) despite the observed defect in the clearance of protein aggregates (Figure 2a). To further evaluate autophagic functions, we examined lysosomal activity by Lysotracker Red staining. Bortezomib similarly stimulated lysosomal acidification in the presence and absence of ST80 (Figure 2c, Supplementary Figure S1c), demonstrating that ST80 does not impair Bortezomib-mediated lysosomal acidification. Taken together, these findings show that ST80/Bortezomib cotreatment triggers the accumulation of insoluble protein aggregates and p62 protein in the subpopulation of cells that survive ST80/Bortezomib cotreatment without impairing the formation of autophagosomes or lysosomal acidification. This points to defective clearance of protein aggregates by the ongoing autophagy, consistent with impaired transport and removal of protein aggregates upon inhibition of the UPS and HDAC6.

BAG3 is upregulated upon ST80/Bortezomib cotreatment

As ST80/Bortezomib cotreatment triggers accumulation of potentially toxic protein aggregates, we hypothesized that the cotreatment simultaneously engages a rescue mechanism in surviving cells to mitigate proteotoxic stress, thereby allowing cells to recover. As the co-chaperone BAG3 has been reported to be upregulated when proteasomal function declines during aging,[8] we analyzed BAG3 expression levels. Intriguingly, ST80/Bortezomib cotreatment strongly co-operated to increase BAG3 mRNA and protein levels in the subpopulation of RMS cells that survived ST80/Bortezomib cotreatment (Figures 3a–c, Supplementary Figure S2b). Kinetic analysis revealed a delayed increase of BAG3 mRNA levels starting about 30–42 h upon treatment with ST80/Bortezomib (Figure 3d). In contrast to RMS cells, no co-operative upregulation of BAG3 mRNA or protein levels by ST80/Bortezomib cotreatment was observed in non-malignant human fibroblasts, whereas treatment with Bortezomib alone resulted in a slight increase in BAG3 mRNA or protein expression (Supplementary Figures S2a and b).

To confirm the specificity of BAG3 upregulation, we determined in parallel mRNA levels of the co-chaperone BAG1, which has been implicated in protein degradation via the proteasome.[18] In contrast to the marked upregulation of BAG3, ST80/Bortezomib

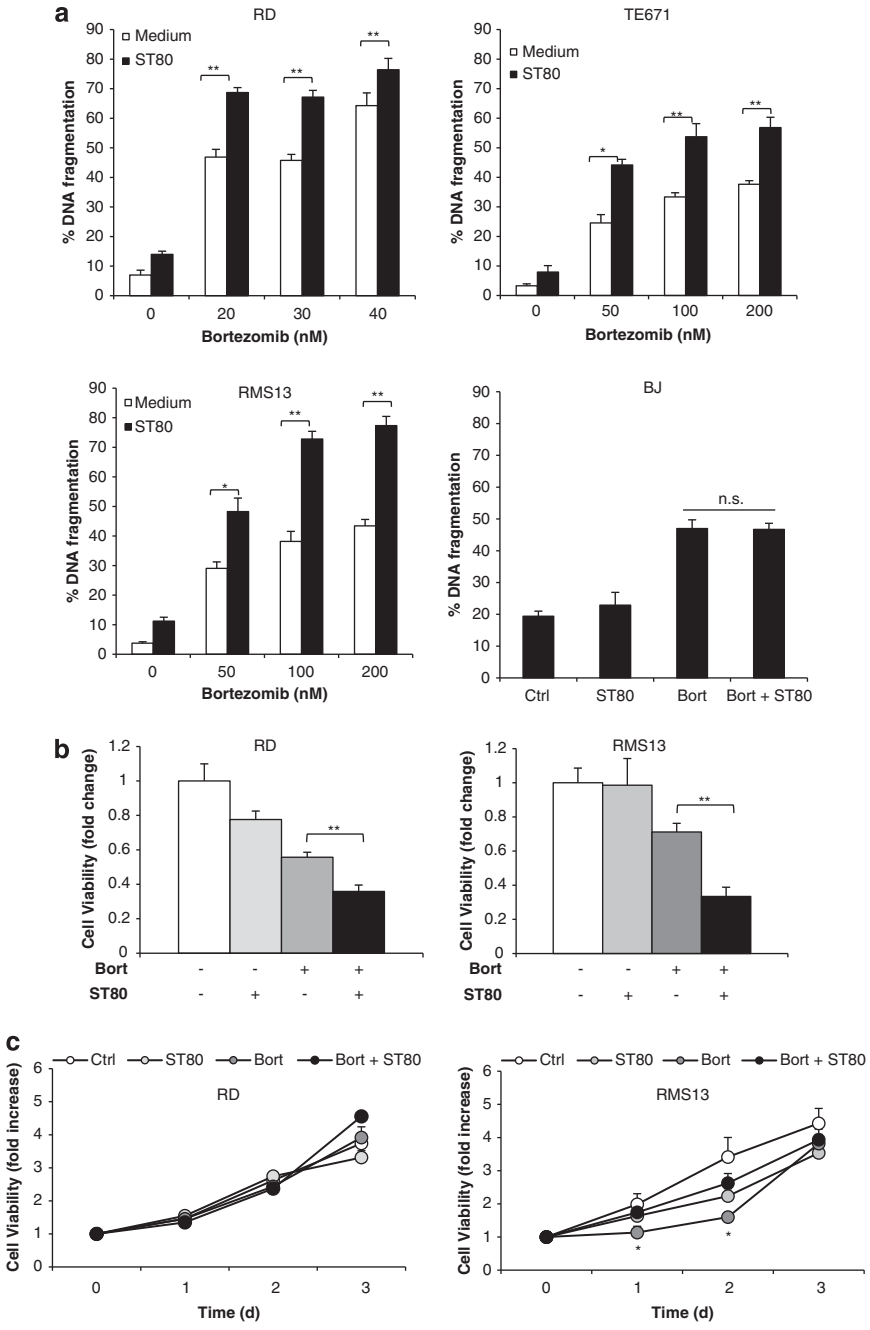

Figure 1. A subpopulation of RMS cells survives and recovers after ST80/Bortezomib cotreatment. (**a**) RMS cells were treated for 48 h with indicated concentrations of Bortezomib and/or 50 μM ST80. BJ fibroblasts were treated for 48 h with 20 nM Bortezomib and/or 50 μM ST80. Apoptosis was determined by fluorescence-activated cell-sorting (FACS) analysis of DNA fragmentation of propidium iodide-stained nuclei. (**b**) RD and RMS13 cells were treated for 48 h with 20 nM (RD) or 50 nM (RMS13) Bortezomib in the presence or absence of 50 μM ST80. Cell viability was measured by crystal violet staining and is expressed as fold change of untreated cells. (**c**) RD and RMS13 cells were treated for 48 h with 20 nM (RD) or 50 nM (RMS13) Bortezomib in the presence or absence of 50 μM ST80, after treatment for 48 h drugs were removed (day 0), and cells were grown in fresh, drug-free medium up to 3 days. Cell viability was measured at indicated time points by crystal violet staining. In (**a**–**c**) mean + s.d. of three independent experiments performed in triplicate are shown; $*P<0.05$; $**P<0.001$ comparing cells treated with Bortezomib in the absence and presence of ST80; n.s., not significant.

cotreatment minimally altered BAG1 mRNA expression (Figure 3a–c). To exclude that BAG3 is simply upregulated as an unspecific stress response to the induction of cell death, we also analyzed BAG3 expression upon treatment with two prototypic apoptotic stimuli, that is, the TRAIL receptor 2 agonistic antibody Lexatumumab, which induces apoptosis in RMS cells via the death receptor (extrinsic) pathway of apoptosis,[19] and the BH3 (Bcl-2 homology domain 3) mimetic ABT-737 that engages the mitochondrial (intrinsic) pathway of apoptosis. Neither treatment with Lexatumumab nor with ABT-737 upregulated BAG3 mRNA levels, although both agents triggered DNA fragmentation to a similar extent compared with ST80/Bortezomib (Supplementary Figures S2c–f). This indicates that BAG3 upregulation is not simply a general feature of apoptotic cells.

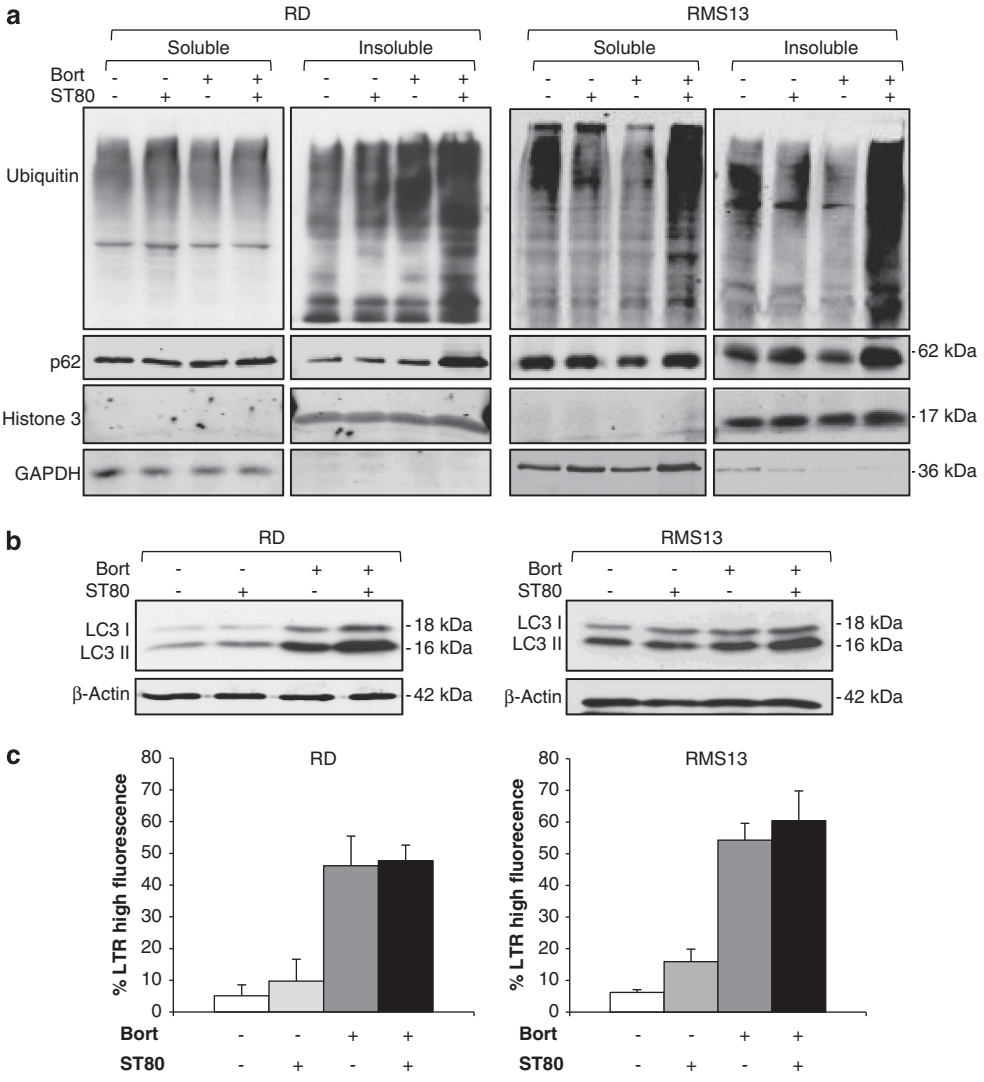

Figure 2. ST80/Bortezomib cotreatment triggers accumulation of insoluble protein aggregates. RD and RMS13 cells were treated for 48 h with 20 nM (RD) or 50 nM (RMS13) Bortezomib and/or 50 μM ST80. (**a**) Ubiquitin-positive protein aggregates were assessed by western blot analysis after fractionation of total viable cells in TritonX-100 (TX-100) into soluble and insoluble fractions. GAPDH and histone 3 were used as loading and purity controls for soluble and insoluble fractions, respectively. (**b**) Autophagosome formation was determined by LC3-I/LC3-II conversion using western blot analysis. β-Actin was used as loading control. (**c**) Lysosomal acidification was quantified by FACS analysis of lysotracker RED-stained cells. Mean + s.d. of three independent experiments performed in triplicate are shown.

Together, these data demonstrate that BAG3 is specifically upregulated in cells which survive proteotoxic stress upon ST80/Bortezomib cotreatment, suggesting that BAG3 may act as a compensatory mechanism to clear protein aggregates upon concomitant inhibition of the proteasome and HDAC6.

BAG3 is required for the clearance of protein aggregates during cell recovery

To investigate whether BAG3 is required for clearing protein aggregates after ST80/Bortezomib cotreatment, we stably knocked down BAG3 by short hairpin RNA (shRNA) vectors. As control, we used a RNA sequence with no corresponding counterpart in the human genome. All three shRNA vectors targeting BAG3 caused downregulation of constitutive BAG3 mRNA and protein levels (Supplementary Figures S3a and b). In addition, silencing of BAG3 prevented the upregulation of BAG3 expression upon ST80/Bortezomib treatment and during the recovery phase after drug removal compared with control vector cells, which maintained high BAG3 levels for several days after drug removal (Figure 4a, Supplementary Figure S3c). Also, we confirmed that BAG3 knockdown did not result in compensatory upregulation of BAG1 levels (Supplementary Figure S3d). To explore whether BAG3 is required for the clearance of protein aggregates during cell recovery, we assessed the amount of protein aggregates and p62 protein at the time of drug removal after cotreatment with ST80/Bortezomib for 48 h (that is, day 0 of recovery) and 2 or 3 days later. Cotreatment with ST80/Bortezomib for 48 h caused comparable accumulation of ubiquitin-positive protein aggregates and p62 protein levels in the insoluble fraction in BAG3 knockdown and control cells (Figure 4b), consistent with the delayed kinetic of BAG3 upregulation starting 30–42 h upon ST80/Bortezomib treatment (Figure 3d). Importantly, in the recovery phase 2 or 3 days after removal of ST80/Bortezomib, silencing of BAG3 caused a marked increase both in protein aggregates and in p62 protein levels in the insoluble fraction compared with control cells (Figure 4c). Similarly, the filter trap assay confirmed that BAG3 knockdown cells maintained higher levels of insoluble protein aggregates 3 days after ST80/Bortezomib removal compared with control cells, while

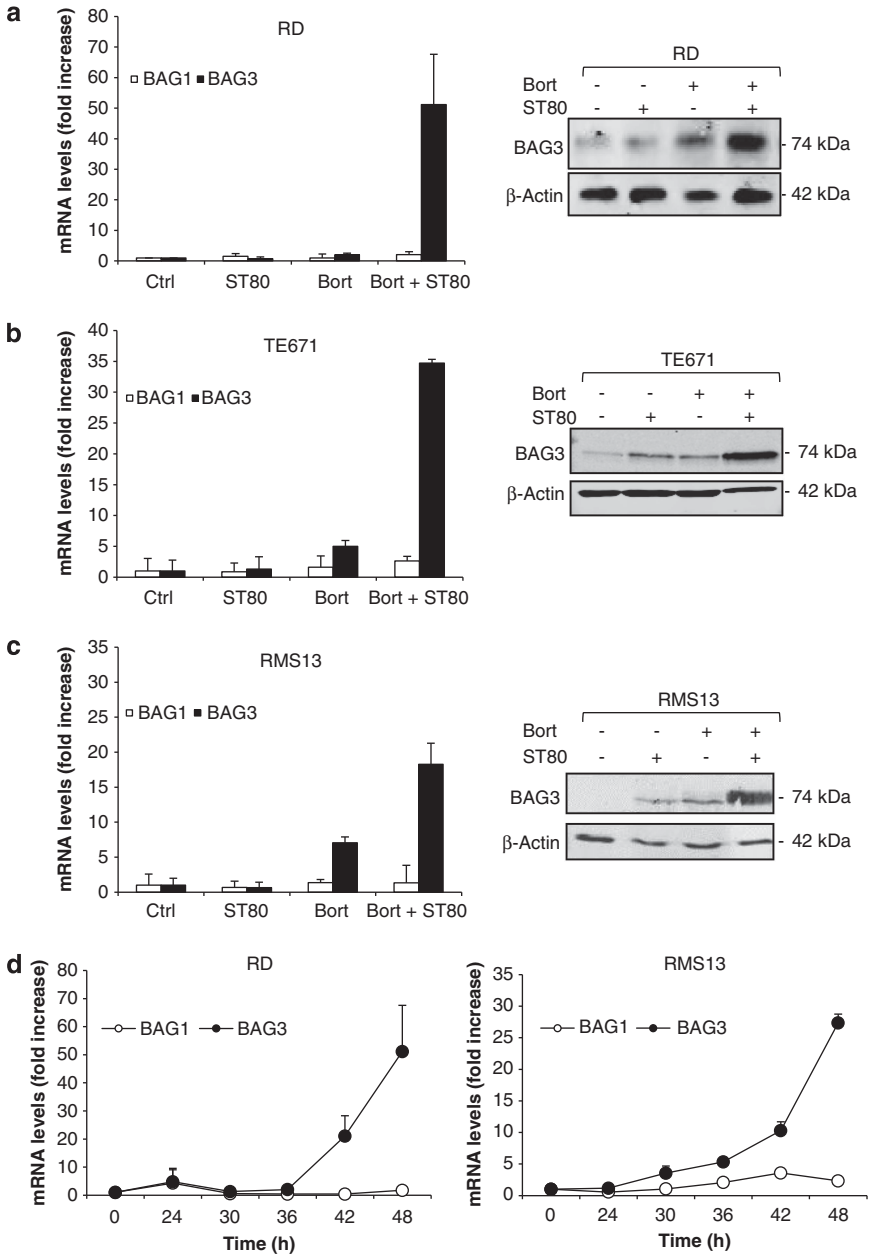

Figure 3. BAG3 is upregulated upon ST80/Bortezomib cotreatment. (**a**–**c**) RMS cells were treated for 48 h with 20 nM (RD) or 50 nM (RMS13, TE671) Bortezomib and/or 50 μM ST80. mRNA levels of BAG1 and BAG3 were assessed by quantitative reverse transcription PCR (qRT–PCR). BAG3 protein levels were determined by western blot analysis. β-Actin was used as loading control. (**d**) RD and RMS13 cells were treated with 20 nM (RD) or 50 nM (RMS13) Bortezomib and 50 μM ST80 for indicated times. mRNA levels of BAG1 and BAG3 were assessed by qRT-PCR. Mean + s.d. of three independent experiments performed in triplicate are shown.

levels of ubiquitin-positive protein aggregates were comparable in BAG3 knockdown and control cells after cotreatment with ST80/Bortezomib for 48 h at day 0 of recovery (Supplementary Figure S3c).

This set of experiments shows that BAG3 is critically required for the clearance of protein aggregates during cell recovery after ST80/Bortezomib cotreatment.

BAG3 is necessary for cell recovery after ST80/Bortezomib cotreatment

Next, we investigated the question whether BAG3 is necessary to mitigate the cytotoxicity of protein aggregates after ST80/Bortezomib cotreatment. To this end, we monitored cell regrowth during recovery after removal of ST80/Bortezomib in BAG3 knockdown and control cells. Strikingly, BAG3 knockdown cells completely failed to regrow during the recovery phase, resulting in reduced cell viability at day 10 compared with day 0 of the recovery phase (Figure 5a). In sharp contrast, shRNA control cells, which upregulated BAG3 upon ST80/Bortezomib treatment (Figure 4a), regrew by several folds upon drug removal (Figure 5a). No significant differences in cell regrowth during recovery were observed between BAG3 knockdown and control cells treated with either ST80 or Bortezomib alone compared with untreated cells (Supplementary Figure S4a), in line with our findings that BAG3 is predominately upregulated in cells exposed to ST80/Bortezomib cotreatment (Figure 3a–c). To explore whether this lack of cell recovery in BAG3 knockdown cells is

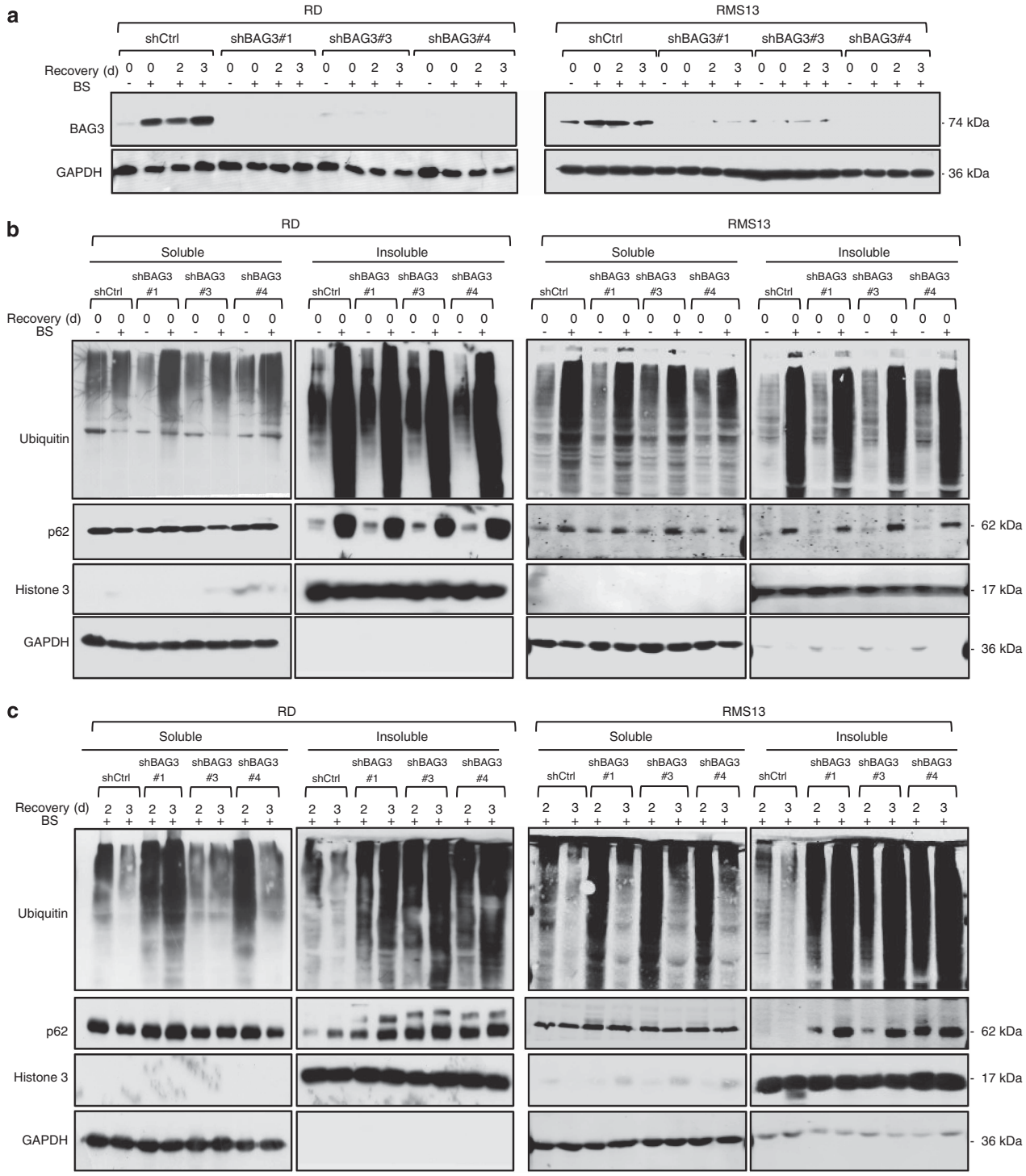

Figure 4. BAG3 is required for the clearance of protein aggregates during cell recovery. RD and RMS13 cells transduced with control vector (shCtrl) or vectors containing three different shRNA sequences against BAG3 were treated for 48 h with 20 nM (RD) or 50 nM (RMS13) Bortezomib and 50 μM ST80 (BS) before treatment was removed (day 0) and cells were grown in fresh, drug-free medium up to 3 days. (**a**) Total BAG3 protein levels were detected by western blot analysis. GAPDH was used as loading control. (**b** and **c**) Ubiquitin-positive protein aggregates were assessed by western blot analysis after fractionation of total viable cells in TX-100 into soluble and insoluble fractions. GAPDH and histone 3 were used as loading and purity controls for soluble and insoluble fractions, respectively.

due to the induction of apoptosis we measured in parallel DNA fragmentation. As shown in Figure 5b, BAG3 knockdown cells exhibited significantly higher amounts of DNA fragmentation 3 days after removal of ST80/Bortezomib compared to control cells.

To examine the effect of BAG3 on clonogenic survival, we determined single cell clonogenic growth during recovery after ST80/Bortezomib cotreatment. To this end, BAG3 knockdown and control cells were treated for 48 h with ST80/Bortezomib. Then,

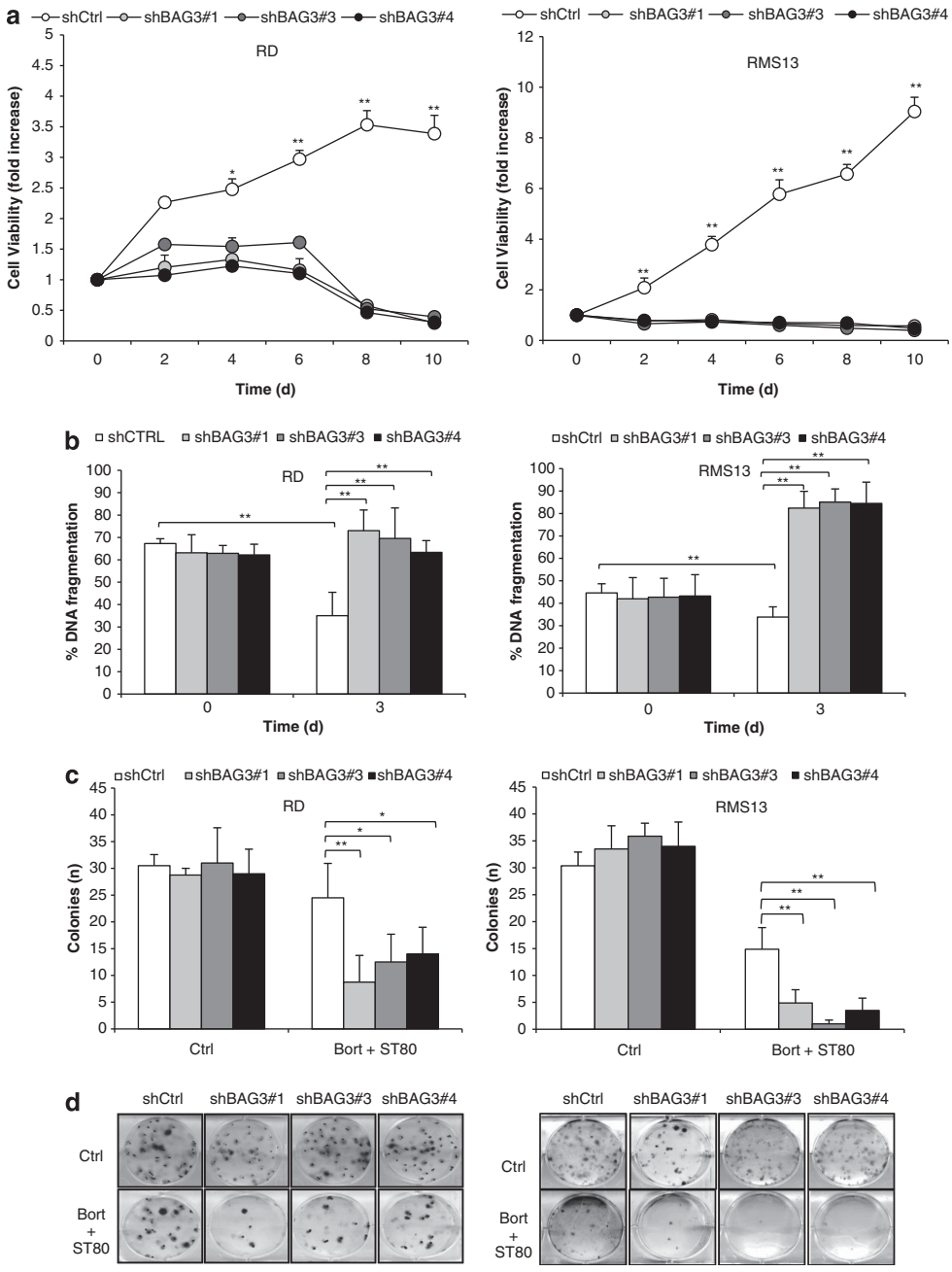

Figure 5. BAG3 is necessary for cell recovery after ST80/Bortezomib cotreatment. RD and RMS13 cells transduced with control vector (shCtrl) or vectors containing three different shRNA sequences against BAG3 were treated for 48 h with 20 nM (RD) or 50 nM (RMS13) Bortezomib and 50 μM ST80 (BS) before treatment was removed (day 0), and cells were grown in fresh, drug-free medium. (**a**) Cell viability was measured at indicated time points by crystal violet staining. (**b**) Apoptosis was determined by FACS analysis of DNA fragmentation of propidium iodide-stained nuclei. (**c** and **d**) After 48 h treatment with ST80/Bortezomib cells were seeded as single cells and grown in drug-free medium for 14 days before colony formation was assessed by crystal violet staining and colonies were counted under the microscope. The number of colonies (**c**) and representative images (**d**) are shown. Mean + s.d. of three independent experiments performed in triplicate (**a** and **b**) or duplicate (**c**) are shown; $*P<0.05$; $**P<0.001$ comparing shCtrl and shBAG3 cells.

surviving cells were seeded as single cells in drug-free medium and the number of colonies was assessed after 14 days. Importantly, BAG3 knockdown significantly reduced colony formation of cells that survived ST80/Bortezomib cotreatment compared with control vector cells (Figures 5c and d). No significant difference in colony formation was detectable between untreated BAG3 knockdown and control vector cells (Figure 5c), indicating that basal BAG3 levels are dispensable for colony growth of RMS cells in the absence of proteotoxic stress. Also, BAG3 knockdown did not alter ST80/Bortezomib-induced apoptosis during the initial 48 h treatment period with ST80/Bortezomib compared with control cells (Supplementary Figure S4b), in line with the delayed kinetic of BAG3 upregulation starting 30–42 h of ST80/Bortezomib treatment (Figure 3d).

This set of experiments demonstrates that BAG3 is critically required during the recovery phase after ST80/Bortezomib cotreatment to support cell regrowth and clonogenic survival and to reduce cell death.

Inhibition of autophagosome formation impairs clearance of protein aggregates and recovery of cells surviving ST80/Bortezomib cotreatment

As BAG3-mediated clearance of protein aggregates has previously been associated with selective autophagy,[20] we hypothesized that autophagy is required for the removal of protein aggregates after ST80/Bortezomib treatment. To address this question, we interfered with the induction of autophagy selectively during the recovery phase after drug removal of ST80/Bortezomib by generating cells with inducible knockdown of autophagy-related protein 7 (ATG7). Downregulation of ATG7 was detectable after 48 h exposure to doxycycline (that is, day 0 of recovery) and sustained at least for up to 120 h (that is, day 3 of recovery; Figure 6a, Supplementary Figure S5a). Downregulation of ATG7 was accompanied by reduced LC3-II conversion (Figure 6a), demonstrating that ATG7 knockdown impairs autophagosome formation under basal conditions. Importantly, ATG7 knockdown substantially delayed the clearance of protein aggregates and of p62 protein at day 2 and 3 of recovery after ST80/Bortezomib cotreatment compared with control cells (Figure 6b). Also, silencing of ATG7 significantly impaired cell regrowth during recovery after ST80/Bortezomib cotreatment compared with control cells, resulting in a substantial reduction of cell viability at day 2 and 3 compared with day 0 of the recovery period and increased apoptosis (Figures 6c and d). In contrast, control cells showed a marked increase in cell growth and reduced apoptosis upon drug removal (Figures 6c and d). By comparison, cells with inducible ATG7 knockdown showed no differences in ST80/Bortezomib-triggered apoptosis or loss of cell viability compared with control cells during the initial treatment with ST80 and Bortezomib for 48 h (Supplementary Figures S5d and e), in line with the delayed kinetic of ATG7 downregulation observed 48 h after the addition of doxycycline (Supplementary Figure S5a).

As a side note, we detected a slight but significant decrease in basal cell growth in ATG7 knockdown compared with control cells also in the absence of ST80/Bortezomib (Supplementary Figure S5b), in line with the role of basal autophagy in maintaining cancer cell viability. However, this slight difference in constitutive cell growth cannot fully explain the marked difference in cell viability between ATG7 knockdown and control cells at day 3 of recovery after ST80/Bortezomib cotreatment (Supplementary Figure S5b, Figure 6c). This indicates that autophagy is required to support viability of RMS cells in particular after proteotoxic stress and to some extent under basal conditions.

Together, this set of experiments shows that inhibition of autophagosome formation prevents clearance of protein aggregates and impairs cell regrowth during recovery after ST80/Bortezomib cotreatment similarly to silencing of BAG3.

Inhibition of lysosomal degradation impairs clearance of protein aggregates and recovery of cells surviving ST80/Bortezomib cotreatment

Finally, we investigated the requirement of the aggresome-autophagy system for cell recovery after ST80/Bortezomib cotreatment by inhibiting lysosomal degradation, which is required for the removal of the cargo during autophagy. To this

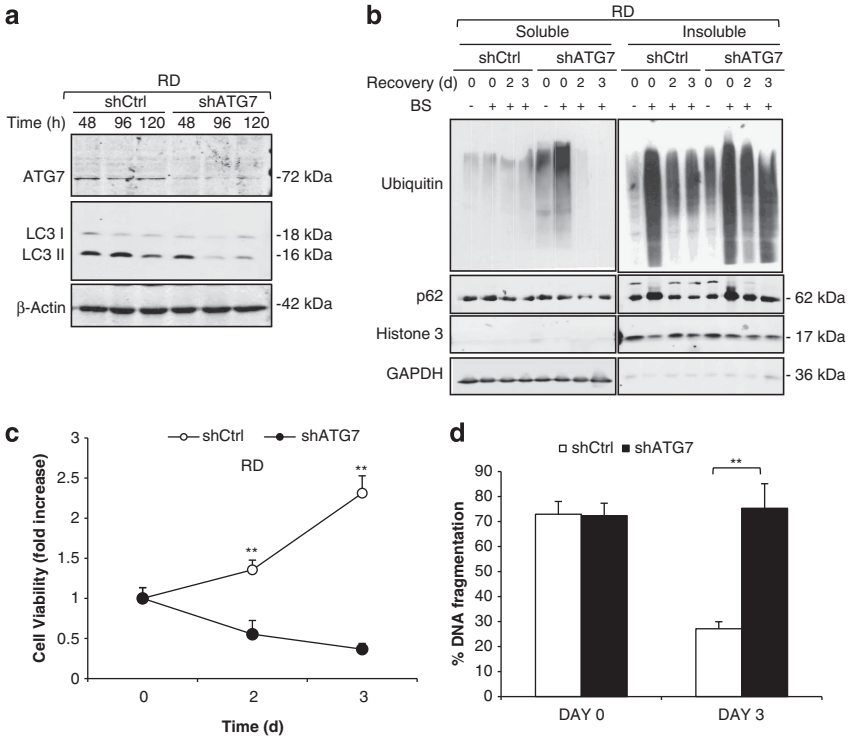

Figure 6. Inhibition of autophagosome formation impairs clearance of protein aggregates and recovery of cells surviving ST80/Bortezomib cotreatment. RD cells were transduced with an inducible vector containing a shRNA sequence against ATG7 (shATG7) or control vector (shCtrl). (**a**) Knockdown efficiency was evaluated at indicated time points by western blot analysis of ATG7 and LC3-I/II conversion after treatment with 1 μg/ml doxycycline. β-Actin was used as loading control. (**b**–**d**) Cells were treated with 20 nM Bortezomib and 50 μM ST80 for 48 h (BS) before treatment was removed (day 0), and cells were grown in fresh, drug-free medium up to 3 days. In (**b**), ubiquitin-positive protein aggregates were assessed by western blot analysis after fractionation of total viable cells in TX-100 into soluble and insoluble fractions. GAPDH and histone 3 were used as loading and purity controls for soluble and insoluble fractions, respectively. In (**c**), cell viability was measured at indicated time points by crystal violet staining. In (**d**), apoptosis was determined by FACS analysis of DNA fragmentation of propidium iodide-stained nuclei. Mean + s.d. of three independent experiments performed in triplicate are shown; $^{**}P < 0.001$ comparing control to ATG7 knockdown cells.

end, we used Bafilomycin A1 (BafA1), a specific V-ATPase inhibitor that blocks lysosomal acidification and thereby lysosomal degradation. Of note, the addition of BafA1 substantially impaired clearance of insoluble protein aggregates during recovery at days 2 and 3 after removal of ST80/Bortezomib, accompanied by an increase of p62 protein levels (Figure 7a). Importantly, BafA1 significantly reduced cell regrowth and increased apoptosis after ST80/Bortezomib treatment (Figures 7b and c). These findings confirm that a functional autophagic/lysosomal degradation system is required for the removal of protein aggregates and cell regrowth during recovery after ST80/Bortezomib treatment.

DISCUSSION

Concomitant inhibition of constitutive protein degradation pathways using proteasome and HDAC inhibitors has recently been suggested as a promising strategy to trigger cancer cell death via enhanced proteotoxicity.[21] As we observed that a substantial subpopulation of RMS cells survives this cotreatment and can even recover and regrow after drug removal, we investigated the underlying escape mechanism in the current study. Here, we identify the co-chaperone BAG3 as a key mediator of inducible resistance after ST80/Bortezomib-induced proteotoxic stress that mitigates proteotoxicity by promoting clearance of protein aggregates via autophagy. This conclusion is supported by several independent lines of evidence (Figure 8). First, ST80 and Bortezomib co-operatively upregulate BAG3 mRNA and protein levels in RMS cells, which survive ST80/Bortezomib cotreatment, in parallel with the accumulation of insoluble, ubiquitin-positive protein aggregates. Second, BAG3 is critically required to clear protein aggregates and to support cell regrowth during the recovery period after removal of ST80/Bortezomib by engaging autophagy, as BAG3 knockdown severely impairs clearance of protein aggregates, significantly increases cell death and reduces long-term viability and clonogenic growth during recovery. Third, blockage of the autophagic pathway, either by genetic inhibition of autophagosome formation via ATG7

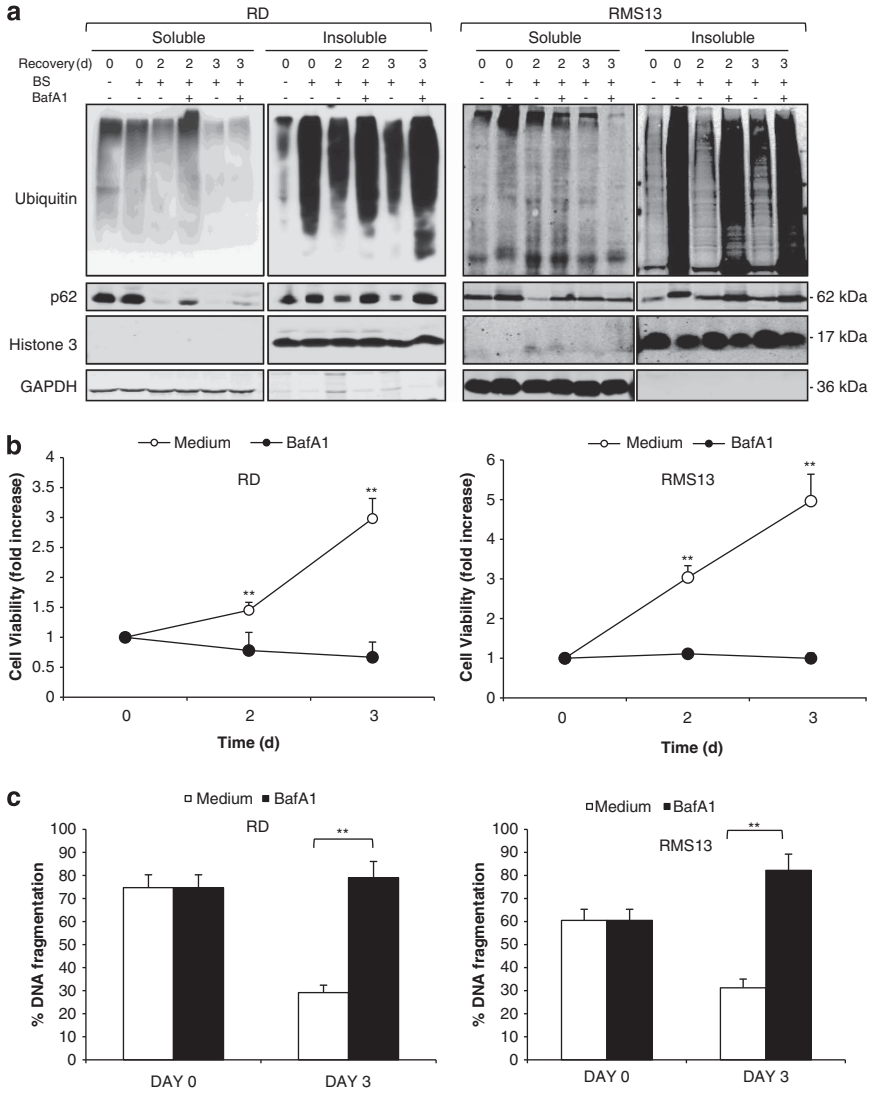

Figure 7. Inhibition of lysosomal degradation impairs clearance of protein aggregates and recovery of cells surviving ST80/Bortezomib cotreatment. RD and RMS13 cells were treated for 48 h with 20 nM (RD) or 50 nM (RMS13) Bortezomib and 50 μM ST80 (BS) before treatment was removed (day 0), and cells were grown in fresh medium with or without 5 nM Bafilomycin A1 up to 3 days. (**a**) Ubiquitin-positive protein aggregates levels were assessed by western blot analysis after fractionation of total viable cells in TX-100 into soluble and insoluble fractions. GAPDH and histone 3 were used as loading and purity controls for soluble and insoluble fractions, respectively. (**b**) Cell viability was measured at indicated time points by crystal violet staining. (**c**) Apoptosis was determined by FACS analysis of DNA fragmentation of propidium iodide-stained nuclei. Mean + s.d. of three independent experiments performed in triplicate are shown; $^{**}P<0.001$ comparing cells in the presence and absence of Bafilomycin A1.

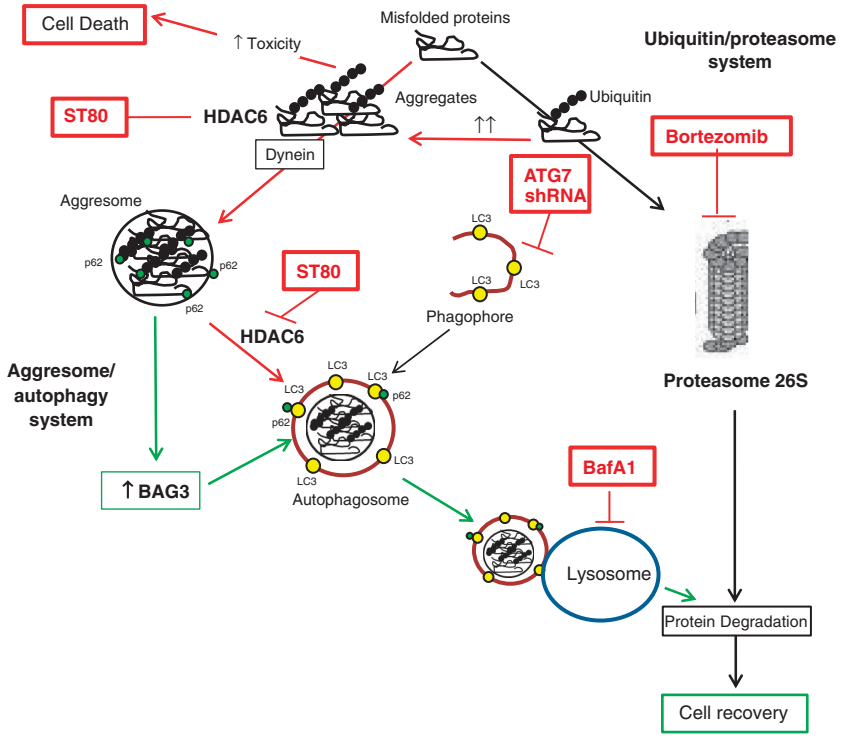

Figure 8. Scheme of the proposed mechanism. Inhibition of HDAC6 and of the proteasome by ST80/Bortezomib cotreatment co-operates to trigger cell death and causes accumulation of protein aggregates (red). Cells that survive ST80/Bortezomib cotreatment upregulate BAG3, which enhances clearance of protein aggregates via the aggresome-autophagy system, thereby decreasing toxicity and promoting cell recovery (green).

knockdown or by pharmacological inhibition of lysosomal degradation using the V-ATPase pump inhibitor BafA1, impairs the clearance of protein aggregates and significantly reduces cell regrowth during recovery upon drug removal. Thus, BAG3-mediated selective autophagy serves as an on-demand, compensatory PQC pathway that is induced upon simultaneous inhibition of the two major constitutive protein degradation pathways, and critically required to mitigate proteotoxic stress by removing accumulated protein aggregates.

BAG3 has been described to promote protein degradation via the aggresome/autophagy pathway via interaction with several proteins involved in this process.[22] As co-chaperone, it mediates the recognition and binding of the HSPB8-HSP70-CHIP-BAG3 multichaperone complex to misfolded proteins.[9] Also, BAG3 interacts with dynein and stimulates substrate transfer from HSP70 to the dynein motor complex via its nucleotide-exchange factor activity, thereby promoting the retrograde transport of misfolded proteins along microtubules to the microtubule organizing center to form insoluble protein aggregates and aggresomes.[8] Furthermore, BAG3 binds to the selective autophagy receptor p62 that links ubiquitinated substrates to the autophagy marker protein LC3 on autophagosomal membranes, thereby targeting misfolded proteins to autophagosomes for their degradation via selective autophagy.[8] Also, BAG3 has recently been reported to mediate selective autophagy of misfolded proteins independently of substrate ubiquitination.[23]

The novelty of our study resides in particular in the identification of BAG3 as a key mediator of an inducible, compensatory PQC pathway to support RMS cell survival in response to concomitant blockade of basal PQC pathways by ST80/Bortezomib cotreatment. Concomitant pharmacological inhibition of the proteasome and HDAC6 has recently been suggested to be superior to treatment with proteasome inhibitors alone to trigger cell death in cancer cells, as inefficient degradation by one of the two major constitutive pathways for protein turnover is often compensated by increased protein degradation by the other system.[21] To this end, proteasome inhibitors such as Bortezomib together with HDAC inhibitors have demonstrated synergistic cytotoxicity in several cancers, for example, ovarian, breast and colon carcinoma.[11–13] Although we similarly show in RMS that cotreatment with ST80 and Bortezomib co-operates to trigger cell death, our present study focused on the surviving, but not the dying cell subpopulation, as we aimed at identifying the mechanism of acquired resistance to ST80/Bortezomib-induced proteotoxic stress. Notably, we demonstrate for the first time that BAG3-mediated autophagy is turned on as a compensatory pathway upon concomitant inhibition of the proteasome and HDAC6 that is required for clearance of protein aggregates and cell regrowth during recovery after proteotoxic stress. This indicates that BAG3 upregulation represents an important inducible resistance mechanism in the context of therapeutic inhibition of the two major constitutive protein degradation pathways in cancer cells. Of note, our data show that BAG3 is necessary to support the survival of RMS cells during the recovery phase after drug removal, while it is dispensable during the initial 48 h treatment period with ST80/Bortezomib. This differential role of BAG3 during the recovery period is consistent with the delayed kinetic of BAG3 upregulation in our experiments, as BAG3 mRNA levels start to increase upon 30–42 h of exposure to ST80/Bortezomib. Although NF-κB activity has been implicated in transcriptional upregulation of BAG3 after heat shock,[24] additional studies are required to explore the question whether this transcriptional factor is involved in the current model.

Constitutive BAG3 expression has been detected in several types of human cancers, such as glioblastoma, pancreatic carcinoma, leukemia and thyroid carcinoma, compared with very low basal levels of BAG3 in non-malignant cells.[25–28] Previously, BAG3 has been reported to support cancer cell survival by counteracting apoptosis. For example, BAG3 was shown to co-operate with the chaperone HSP70 to retain Bcl-2-associated X protein, BAX protein in the cytosol, which in turn prevented

Bcl-2-associated X protein translocation to the mitochondria and inhibited cisplatinum- or serum deprivation-induced apoptosis.[25] In addition, BAG3 was described to interfere with the HSP70-mediated delivery of antiapoptotic proteins, such as IKKγ, MCL1, BCL2, BCL-X_L to the proteasome by competing with BAG1 that functions as co-chaperone of HSP70 in this process.[29–31] Compared with these previous reports on the antiapoptotic properties of BAG3, we demonstrate in the present study that BAG3 maintains cancer cell viability by promoting autophagic clearance of protein aggregates. While BAG3 upregulation has been described to confer resistance to treatment with proteasome inhibitors alone,[32,33] we found that BAG3 is dispensable for RMS cell viability upon single agent treatment with Bortezomib, in line with little upregulation of BAG3 by Bortezomib alone compared with ST80/Bortezomib cotreatment in our study.

Induction of BAG3 expression has previously been implicated in other models of PQC during chronic or acute stress due to the accumulation of misfolded or damaged proteins. For example, during aging a BAG1/BAG3-switch has been reported to compensate for the age-dependent decrease in the efficacy of BAG1-mediated proteasomal degradation by engaging BAG3-mediated autophagy as an on-demand selective autophagy pathway.[8] Furthermore, the BAG3-selective autophagy pathway has been implicated in regulating the removal of misfolded protein aggregates in neurodegenerative diseases.[8,34] In addition, upregulation of BAG3 was recently shown to mediate the removal of damaged proteins after heat shock.[24] Our present study adds a new aspect to this concept of BAG3 as an on-demand, inducible PQC system in situations of acute and chronic stress by showing for the first time that BAG3-mediated selective autophagy is induced upon concomitant pharmacological blockade of the two major constitutive branches for protein degradation in cancer cells and critically required to support the recovery from proteotoxic stress.

Our findings have important implications for a better understanding of the molecular regulation of constitutive and inducible PQC pathways in cancer cells. As inhibition of protein degradation is considered as an attractive anticancer strategy,[10] further insights into the mechanisms that regulate sensitivity and resistance of cancer cells to inhibitors of PQC pathways will be critical to exploit this strategy in human cancers. By identifying the BAG3-mediated selective autophagy pathway as a novel mechanism of acquired resistance that compensates for inhibition of the constitutive protein degradation systems, our findings suggest that interfering with this inducible escape mechanism may potentiate the efficacy of protein degradation inhibitors. Thus, inhibition of both inducible and constitutive PQC pathways may open new perspectives for their therapeutic exploitation in cancers.

MATERIALS AND METHODS

Cell culture and chemicals

RMS cell lines and the human fibroblast cell line BJ were obtained from the American Type Culture Collection (Manassas, VA, USA). Cells were maintained in Roswell Park Memorial Institute medium 1640 or Dulbecco's Modified Eagle Medium medium (Life Technologies Inc., Carlsbad, CA, USA), supplemented with 10% fetal calf serum (Biochrom, Berlin, Germany), 1 mM glutamine (Invitrogen, Karlsruhe, Germany), 1% penicillin/streptomycin (Invitrogen) and 25 mM HEPES (Biochrom). Bortezomib was purchased by Jansen-Cilag (Neuss, Germany); Bafilomycin A1 (Baf A1) from Sigma (Deisenhofen, Germany); Doxycycline monohydrate by Santa Cruz Biotechnology (Santa Cruz, CA, USA). ST80[15] was kindly provided by M Jung and Lexatumumab, a fully human agonist monoclonal antibody against TRAIL-R2, by R Humphreys (Human Genome Sciences, Rockville, MD, USA).[35] Chemicals were purchased from Sigma unless otherwise indicated.

RNA interference

For stable or inducible gene knockdown, HEK293T producer cells were transfected with 7.5 μg pGIPZ-shRNAmir or pTRIPZ-shRNAmir vector (Thermo Fisher Scientific, Dreieich, Germany), 12.5 μg pCMV-dR8.91[36] and 1 μg pMD2.G (Addgene no. 12259) using calcium phosphate transfection as previously described[37] (non-silencing control: RHS4346, shBAG3 no. 1: RHS4430; shBAG3 no. 3: RHS4430; shBAG3 no. 4: RHS4430; shATG7: RHS4430).

Determination of apoptosis, cell viability, colony formation and lysosomal acidification

Apoptosis was determined by fluorescence-activated cell-sorting analysis of DNA fragmentation of propidium iodide-stained nuclei as described previously[38] using fluorescence-activated cell-sorting Canto II (BD Biosciences, Heidelberg, Germany). Cell viability was assessed by crystal violet staining (0.75% crystal violet, 50% ethanol, 0.25% NaCl, 1.57% formaldehyde). Crystal violet dye was resolubilized in 1% SDS and absorbance at 550 nM was measured by microplate reader (Infinite M200, Tecan Group Ltd., Maennedorf, Switzerland). For colony assay, cells were treated for 48 h, re-seeded as single cells (200 cells/well) in six-well plates and cultured for additional 14 days before colonies were stained with crystal violet. The number of colonies was counted under the microscope. Lysosomal acidification was determined by staining with 0.05 nM Lysotracker Red (Invitrogen) and flow cytometry according to the manufacturer's instructions.

Western blot analysis

Western blot analysis was performed as described previously[38] using the following antibodies: rabbit anti-p62/SQSTM1 (MBL, Nagoya, Japan); rabbit anti-LC3 (Thermo Scientific, Waltham, MA, USA); rabbit anti-ATG7 and rabbit anti-BAG3 (AbCam, Cambridge, UK); mouse anti-polyubiquitin antibody (Millipore, Darmstadt, Germany). Mouse anti-β-Actin (Sigma), mouse anti-GAPDH (HyTest, Turku, Finland) or rabbit anti-Histone 3 (AbCam) were used as loading controls. Goat anti-mouse immunoglobulin G and goat anti-rabbit immunoglobulin G conjugated to horseradish peroxidase (Santa Cruz Biotechnology) as secondary antibodies and enhanced chemiluminescence were used for detection (Amersham Bioscience, Freiburg, Germany). Alternatively, infrared dye-labeled secondary antibodies and infrared imaging were used for detection (Odyssey imaging system, LI-COR Bioscience, Bad Homburg, Germany). Representative blots of at least two independent experiments are shown.

Determination of protein aggregates

Protein aggregates were determined by fractioning cell lysates in TritonX-100 soluble and insoluble fractions as previously described.[39] Briefly, cells were harvested with cold 1x phosphate-buffered saline and collected by centrifugation (1800 r.p.m.; 5 min). Cell pellets were resuspended in 2% TritonX-100/1x phosphate-buffered saline solution supplemented with protease and phosphates inhibitors, incubated on ice for 30 min. After centrifugation for 30 min at 4 °C and 13 000 r.p.m., the supernatant was recovered as soluble fraction. Pellets were resuspended in 1% SDS supplemented with protease and phosphatase inhibitors and sonicated for 20 s. Expression of ubiquitin-positive proteins was determined by western blot analysis.

Determination of protein aggregates by filter trap assay was performed as previously described.[40] Briefly, protein lysates were solubilized in 1% SDS and directly spotted onto nitrocellulose membrane. Vacuum blotting was performed for 30 min by gel dryer (Bio-Rad, Munich, Germany). Expression of ubiquitin-positive protein aggregates was assessed by staining of the membrane with mouse anti-polyubiquitin antibody (Millipore), followed by goat anti-mouse immunoglobulin G secondary antibody conjugated to horseradish peroxidase (Santa Cruz Biotechnology). Enhanced chemiluminescence (Amersham Bioscience) was used for detection.

Quantitative reverse transcription PCR

Total RNA was extracted using peqGOLD Total RNA kit from Peqlab Biotechnologie GmbH (Erlangen, Germany) according to the manufacturer's instructions. Three micrograms of total RNA were used to synthetize the corresponding complementary DNA using RevertAid H Minus First Strand complementary DNA Synthesis Kit (MBI Fermentas GmbH, St Leon-Rot, Germany). To quantify gene expression levels, SYBR-Green based quantitative reverse transcription PCR was performed using the 7900HT fast real-time PCR system from Applied Biosystems (Darmstadt, Germany) according to manufacturer's instructions. Data were normalized on 18S-rRNA expression as reference gene. The following primers (10 pmol/μl) were used: *BAG1-for*: 5′-TCACCCACAGCAATGAGAAG-3′; *BAG1-rew*: 5′-ATTAACATGACCCGGCAACC-3′; *BAG3-for*: 5′-CTCCATTCCGG

TGATACACGA-3′; *BAG3-rew*: 5′-TGGTGGGTCTGGTACTCCC-3′. Melting curves were plotted to verify the specificity of the amplified products. All determinations were performed in triplicate. The relative expression of the target gene transcript and reference gene transcript was calculated as $\Delta\Delta C_t$.

Statistical analysis

Statistical significance was assessed by Student's *t*-test (two-tailed distribution, two- sample, unequal variance).

CONFLICT OF INTEREST

The authors declare no conflict of interest.

ACKNOWLEDGEMENTS

We thank C Hugenberg for expert secretarial assistance. This work has been partially supported by grants from the Wilhelm-Sander Stiftung, the Deutsche Krebshilfe and the Bundesministerium für Bildung und Forschung (01GM1104C) (to S F). Work on HDAC inhibitors in the Jung group is supported by the Deutsche Forschungsgemeinschaft (JU 295/9-1 within SPP1463, JU 295/10-2 within CRU 201).

REFERENCES

1 Kubota H. Quality control against misfolded proteins in the cytosol: a network for cell survival. *J Biochem* 2009; **146**: 609–616.
2 Kawaguchi Y, Kovacs JJ, McLaurin A, Vance JM, Ito A, Yao TP. The deacetylase HDAC6 regulates aggresome formation and cell viability in response to misfolded protein stress. *Cell* 2003; **115**: 727–738.
3 Lee JY, Koga H, Kawaguchi Y, Tang W, Wong E, Gao YS *et al.* HDAC6 controls autophagosome maturation essential for ubiquitin-selective quality-control autophagy. *Embo J* 2010; **29**: 969–980.
4 Nakatogawa H, Suzuki K, Kamada Y, Ohsumi Y. Dynamics and diversity in autophagy mechanisms: lessons from yeast. *Nat Rev Mol Cell Biol* 2009; **10**: 458–467.
5 Behrends C, Fulda S. Receptor proteins in selective autophagy. *Int J Cell Biol* 2012; **2012**: 673290.
6 Yao TP. The role of ubiquitin in autophagy-dependent protein aggregate processing. *Genes & cancer* 2010; **1**: 779–786.
7 Lamark T, Johansen T. Aggrephagy: selective disposal of protein aggregates by macroautophagy. *Int J Cell Biol* 2012; **2012**: 736905.
8 Gamerdinger M, Hajieva P, Kaya AM, Wolfrum U, Hartl FU, Behl C. Protein quality control during aging involves recruitment of the macroautophagy pathway by BAG3. *Embo J* 2009; **28**: 889–901.
9 Carra S, Seguin SJ, Lambert H, Landry J. HspB8 chaperone activity toward poly(Q)-containing proteins depends on its association with Bag3, a stimulator of macroautophagy. *J Biol Chem* 2008; **283**: 1437–1444.
10 Frankland-Searby S, Bhaumik SR. The 26S proteasome complex: an attractive target for cancer therapy. *Biochim Biophys Acta* 2012; **1825**: 64–76.
11 Bazzaro M, Lin Z, Santillan A, Lee MK, Wang MC, Chan KC *et al.* Ubiquitin proteasome system stress underlies synergistic killing of ovarian cancer cells by bortezomib and a novel HDAC6 inhibitor. *Clin Cancer Res* 2008; **14**: 7340–7347.
12 Carew JS, Medina EC, Esquivel 2nd JA, Mahalingam D, Swords R, Kelly K *et al.* Autophagy inhibition enhances vorinostat-induced apoptosis via ubiquitinated protein accumulation. *J Cell Mol Med* 2010; **14**: 2448–2459.
13 Milani M, Rzymski T, Mellor HR, Pike L, Bottini A, Generali D *et al.* The role of ATF4 stabilization and autophagy in resistance of breast cancer cells treated with Bortezomib. *Cancer Res* 2009; **69**: 4415–4423.
14 Bersani F, Taulli R, Accornero P, Morotti A, Miretti S, Crepaldi T *et al.* Bortezomib-mediated proteasome inhibition as a potential strategy for the treatment of rhabdomyosarcoma. *Eur J Cancer* 2008; **44**: 876–884.
15 Scott GK, Marx C, Berger CE, Saunders LR, Verdin E, Schafer S *et al.* Destabilization of ERBB2 transcripts by targeting 3′ untranslated region messenger RNA associated HuR and histone deacetylase-6. *Mol Cancer Res* 2008; **6**: 1250–1258.
16 Rodriguez-Gonzalez A, Lin T, Ikeda AK, Simms-Waldrip T, Fu C, Sakamoto KM. Role of the aggresome pathway in cancer: targeting histone deacetylase 6-dependent protein degradation. *Cancer Res* 2008; **68**: 2557–2560.
17 Ding WX, Yin XM. Sorting, recognition and activation of the misfolded protein degradation pathways through macroautophagy and the proteasome. *Autophagy* 2008; **4**: 141–150.
18 Tsukahara F, Maru Y. Bag1 directly routes immature BCR-ABL for proteasomal degradation. *Blood* 2010; **116**: 3582–3592.
19 Basit F, Humphreys R, Fulda S. RIP1 protein-dependent assembly of a cytosolic cell death complex is required for inhibitor of apoptosis (IAP) inhibitor-mediated sensitization to lexatumumab-induced apoptosis. *J Biol Chem* 2012; **287**: 38767–38777.
20 Behl C. BAG3 and friends: co-chaperones in selective autophagy during aging and disease. *Autophagy* 2011; **7**: 795–798.
21 Wu WK, Sakamoto KM, Milani M, Aldana-Masankgay G, Fan D, Wu K *et al.* Macroautophagy modulates cellular response to proteasome inhibitors in cancer therapy. *Drug Resist Updat* 2010; **13**: 87–92.
22 Gamerdinger M, Carra S, Behl C. Emerging roles of molecular chaperones and co-chaperones in selective autophagy: focus on BAG proteins. *J Mol Med* 2011; **89**: 1175–1182.
23 Gamerdinger M, Kaya AM, Wolfrum U, Clement AM, Behl C. BAG3 mediates chaperone-based aggresome-targeting and selective autophagy of misfolded proteins. *EMBO Rep* 2011; **12**: 149–156.
24 Nivon M, Abou-Samra M, Richet E, Guyot B, Arrigo AP, Kretz-Remy C. NF-kappaB regulates protein quality control after heat stress through modulation of the BAG3-HspB8 complex. *J Cell Sci* 2012; **125**: 1141–1151.
25 Festa M, Del Valle L, Khalili K, Franco R, Scognamiglio G, Graziano V *et al.* BAG3 protein is overexpressed in human glioblastoma and is a potential target for therapy. *Am J Pathol* 2011; **178**: 2504–2512.
26 Liao Q, Ozawa F, Friess H, Zimmermann A, Takayama S, Reed JC *et al.* The anti-apoptotic protein BAG-3 is overexpressed in pancreatic cancer and induced by heat stress in pancreatic cancer cell lines. *FEBS Lett* 2001; **503**: 151–157.
27 Chiappetta G, Ammirante M, Basile A, Rosati A, Festa M, Monaco M *et al.* The antiapoptotic protein BAG3 is expressed in thyroid carcinomas and modulates apoptosis mediated by tumor necrosis factor-related apoptosis-inducing ligand. *J Clin Endocrinol Metab* 2007; **92**: 1159–1163.
28 Romano MF, Festa M, Petrella A, Rosati A, Pascale M, Bisogni R *et al.* BAG3 protein regulates cell survival in childhood acute lymphoblastic leukemia cells. *Cancer Biol Ther* 2003; **2**: 508–510.
29 Ammirante M, Rosati A, Arra C, Basile A, Falco A, Festa M *et al.* IKK{gamma} protein is a target of BAG3 regulatory activity in human tumor growth. *Proc Natl Acad Sci USA* 2010; **107**: 7497–7502.
30 Aveic S, Pigazzi M, Basso G. BAG1: the guardian of anti-apoptotic proteins in acute myeloid leukemia. *PLoS One* 2011; **6**: e26097.
31 Zhang Y, Wang JH, Lu Q, Wang YJ. Bag3 promotes resistance to apoptosis through Bcl-2 family members in non-small cell lung cancer. *Oncol Rep* 2012; **27**: 109–113.
32 Wang HQ, Liu HM, Zhang HY, Guan Y, Du ZX. Transcriptional upregulation of BAG3 upon proteasome inhibition. *Biochem Biophys Res Commun* 2008; **365**: 381–385.
33 Du ZX, Zhang HY, Meng X, Gao YY, Zou RL, Liu BQ *et al.* Proteasome inhibitor MG132 induces BAG3 expression through activation of heat shock factor 1. *J Cell Physiol* 2009; **218**: 631–637.
34 Seidel K, Vinet J, Dunnen WF, Brunt ER, Meister M, Boncoraglio A *et al.* The HSPB8-BAG3 chaperone complex is upregulated in astrocytes in the human brain affected by protein aggregation diseases. *Neuropathol Appl Neurobiol* 2012; **38**: 39–53.
35 Humphreys RC, Halpern W. Trail receptors: targets for cancer therapy. *Adv Exp Med Biol* 2008; **615**: 127–158.
36 Zufferey R, Nagy D, Mandel RJ, Naldini L, Trono D. Multiply attenuated lentiviral vector achieves efficient gene delivery *in vivo*. *Nat Biotechnol* 1997; **15**: 871–875.
37 Gonzalez P, Mader I, Tchoghandjian A, Enzenmuller S, Cristofanon S, Basit F *et al.* Impairment of lysosomal integrity by B10, a glycosylated derivative of betulinic acid, leads to lysosomal cell death and converts autophagy into a detrimental process. *Cell Death Differ* 2012; **19**: 1337–1346.
38 Fulda S, Sieverts H, Friesen C, Herr I, Debatin KM. The CD95 (APO-1/Fas) system mediates drug-induced apoptosis in neuroblastoma cells. *Cancer Res* 1997; **57**: 3823–3829.
39 Garcia-Mata R, Bebok Z, Sorscher EJ, Sztul ES. Characterization and dynamics of aggresome formation by a cytosolic GFP-chimera. *J Cell Biol* 1999; **146**: 1239–1254.
40 Wanker EE, Scherzinger E, Heiser V, Sittler A, Eickhoff H, Lehrach H. Membrane filter assay for detection of amyloid-like polyglutamine-containing protein aggregates. *Methods Enzymol* 1999; **309**: 375–386.

Supplementary Information accompanies this paper on the Oncogene website (http://www.nature.com/onc)